ELSEVIER

International Journal of Adhesion & Adhesives 29 (2009) 91–97

International Journal of Adhesion & Adhesives

www.elsevier.com/locate/ijadhadh

Stress analysis of the adhesive resin layer in a reinforced pin-loaded joint used in glass structures

Q.D. To[a,b], Q.-C. He[a,*], M. Cossavella[b], K. Morcant[b], A. Panait[b]

[a]*Université Paris-Est, Laboratoire de Modélisation et Simulation Multi Echelle, FRE 3160, CNRS, 5 Boulevard Descartes, F-77454 Marne-la-Vallée Cedex 2, France*

[b]*Centre Scientifique et Technique du Bâtiment (CSTB), 84 Avenue Jean Jaurès, 77447 Marne-la-Vallée Cedex 2, France*

Accepted 11 January 2008

Available online 26 March 2008

Abstract

A reinforced pin-loaded joint used to assemble elements in a tempered glass structure consists of a steel bolt and a steel ring glued to a glass plate through an adhesive resin layer. The stiffness of a typical resin material is generally much lower than the stiffness of steel or glass. This fact leads us to make the assumption that the stress field in the adhesive resin layer is essentially due to the relative rigid displacements of the steel ring with respect to the glass plate. On the basis of this assumption, an analytical solution is obtained for the stresses in the adhesive resin layer. This solution is compared with and validated by the numerical results obtained by the finite element method.

Keywords: C. Stress analysis; C. Finite element stress analysis; E. Joint design

1. Introduction

In tempered glass structures, pin-loaded connections are frequently employed to assemble different glass elements and ensure the structure integrity. The reinforced pin-loaded joint studied in the present work is composed of a steel bolt (or pin), a steel ring and a thin resin layer (see Fig. 1). The steel ring serves for strengthening the hole in a tempered glass plate and is glued to the latter via the resin layer. An external force is transmitted from the steel bolt to the glass plate through the steel ring and the resin layer. Thus, the steel ring is in direct contact with the steel bolt and prevents the glass plate from high stress concentration.

Pin-loaded connections have been widely and intensively studied (see [1–3] and the references cited therein). However, the stress analysis of the adhesive layers involved in finite structures with pin-loaded connections seems not to have been carried out analytically. This is probably because the finiteness of these structures renders it particulary difficult or even impossible to obtain analytical solutions. By contrast, when plates with pin-loaded connections are infinite, certain analytical solutions are available (see, e.g., [4–7]).

The stiffness and strength of the resin constituting a typical thin adhesive layer are much lower than those of the materials (steel and glass) forming the ring and plate. Experimental observations indicate that cracks in the reinforced pin-loaded joint of a tempered glass plate are mostly initiated inside the thin adhesive layer or at its interfaces with the ring and plate (Fig. 2). Consequently, the stress analysis of the thin adhesive resin layer prior to the occurrence of cracks is essential for preventing the reinforced pin-loaded joint from failure.

The main purpose of this work is to obtain a closed-form solution for the stress field inside the thin adhesive layer. This objective is achieved by exploiting the fact that the resin of which the thin layer is made is much softer than steel and glass. Typically, the Young modulus of the resin is hardly superior to 3 GPa while those of glass and steel are about 70 and 200 GPa, respectively. Due to this high stiffness contrast, we infer that, to within terms of high orders, the strain field in the adhesive layer is generated by

*Corresponding author. Tel.: +33 160 957 786; fax: +33 160 957 799.
E-mail address: Qi-Chang.He@univ-mlv.fr (Q.-C. He).

0143-7496/$ - see front matter © 2008 Elsevier Ltd. All rights reserved.
doi:10.1016/j.ijadhadh.2008.01.008

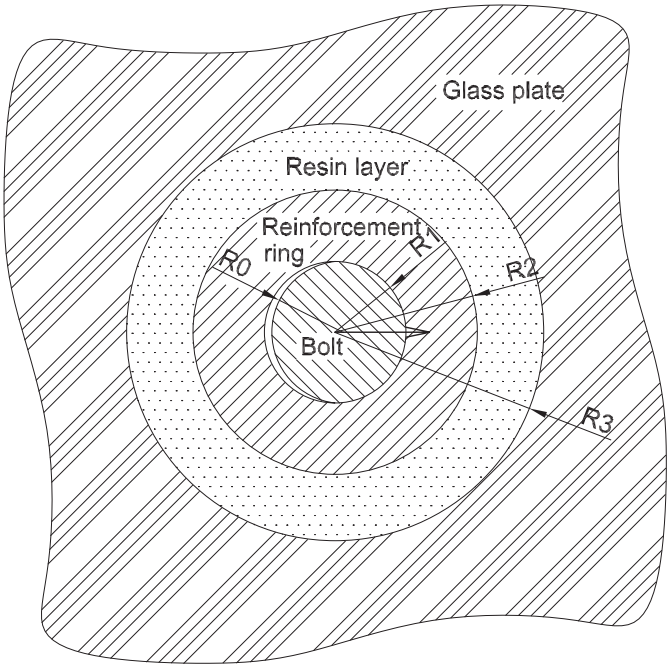

Fig. 1. Composition of a typical reinforced pin-loaded joint in a glass structure.

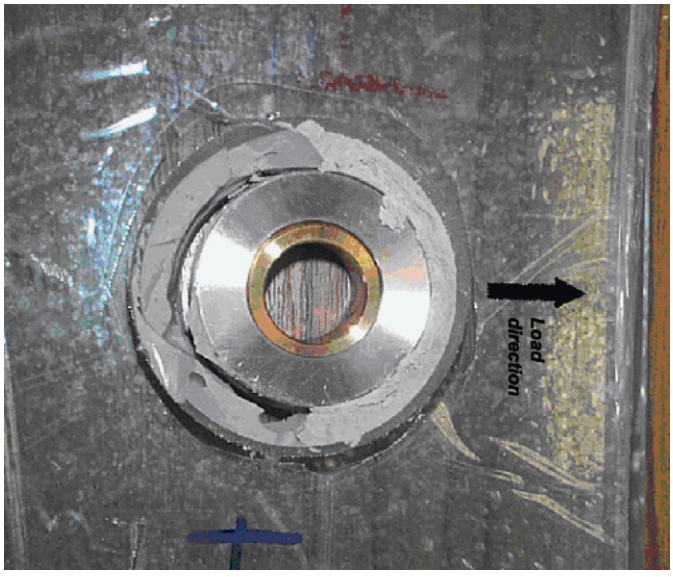

Fig. 2. Failure of the resin of a reinforced pin-loaded joint with the pin put aside.

the relative rigid displacements of the steel ring with respect to the glass plate. In other words, in determining the stress field in the adhesive layer, the ring and plate can be practically taken to be rigid. This assumption considerably simplifies the stress analysis of the adhesive layer in a finite structure involving unilateral contact and friction which are strongly nonlinear phenomena. Indeed, as the ring and glass are considered as rigid, the structure under investigation behaves as an infinite one and the stress field in the adhesive layer does not depend on the exact distribution of the contact stresses on the surface between the bolt and ring but only on the resulting forces of the contact stresses.

To check the validity of the assumption that the steel ring and glass plate act practically as being rigid in analyzing the stresses in the adhesive layer, the finite element method is applied to a glass structure with a reinforced pin-loaded joint where the ring and plate are taken to be linearly isotropic elastic. The results given by our analytical solution for the stresses in the adhesive layer are compared with the relevant results provided by a full numerical simulation based on the finite element method. This comparison shows a good agreement between the results delivered by our analytical solution and the ones issued from the numerical method.

The paper is organized as follows. Section 2 specifies the problem under investigation and determines the stress field inside the adhesive layer by using the aforementioned relative rigid displacement hypothesis. The analytical results derived in Section 2 are compared against and validated by the numerical results obtained by the finite element method in Section 3. A few concluding remarks are drawn in Section 4.

2. Analytical solution for the stress field in the adhesive resin layer

Consider a reinforced pin-loaded joint whose composition is shown in Fig. 1. The components of the joint and their dimensions relative to a system of polar coordinates are specified as follows:

- the steel bolt: $0 \leqslant r \leqslant R_0$;
- the steel ring: $R_1 \leqslant r \leqslant R_2$;
- the adhesive resin layer: $R_2 \leqslant r \leqslant R_3$;
- the glass plate: $r \geqslant R_3$.

Before the occurrence of cracks or plastic strains, the materials constituting the pin, ring, resin and glass are all taken to be linearly elastic and isotropic, so that it is characterized by the Young modulus E_i and Poisson ratio ν_i with $i = 0, 1, 2, 3$ for the pin, ring, resin and glass, respectively. In what follows, we make the assumption of plane elasticity. Thus, it is convenient to introduce Kolosov's constants κ_i and μ_i related to E_i and ν_i by the expressions

$$\mu_i = \frac{E_i}{2(1+\nu_i)}, \quad \kappa_i = \frac{3-\nu_i}{1+\nu_i} \quad \text{(plane stress)},$$
$$\kappa_i = 3 - 4\nu_i \quad \text{(plane strain)}.$$

According as $\kappa_i = (3-\nu_i)/(1+\nu_i)$ or $\kappa_i = 3 - 4\nu_i$ is adopted, the results presented below are valid for the case of plane stress or plane strain. The glass structure under investigation complies with the hypothesis of plane stress.

As argued in the Introduction, owing to the fact that the adhesive resin layer is very soft in comparison with the glass plate and steel reinforcement ring, the determination of the stress field inside the resin layer can be carried out by considering the glass plate and steel ring as rigid bodies. In

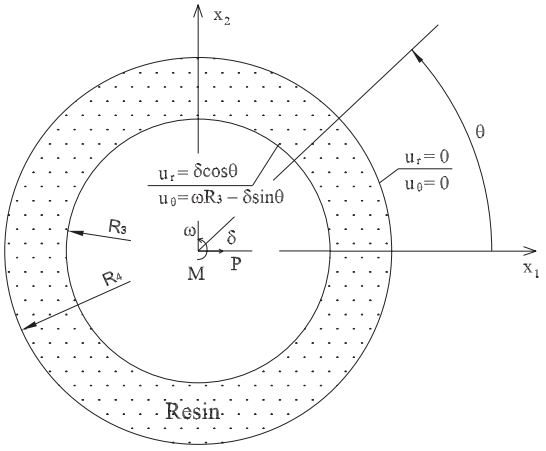

Fig. 3. Boundary conditions for the adhesive resin layer.

other words, their interfaces with the resin layer can be admitted as undeformable and the stress field inside the resin layer depends only on their relative displacements (i.e. relative translation and rotation) caused by external loadings. So, let us examine the case where the resultant forces transmitted from the bolt to the ring correspond to a horizontal force P and a moment M applied at the origin O, which cause a relative horizontal translation δ and a relative rotation ω between the two interfaces (see Fig. 3). The boundary conditions for the resin layer can be written in the polar coordinate system as follows:

$$\begin{aligned} &u_r(R_3,\theta)=u_\theta(R_3,\theta)=0, \quad \forall\theta\in[-\pi,\pi],\\ &u_r(R_2,\theta)=\delta\cos\theta,\\ &u_\theta(R_2,\theta)=\omega R_2-\delta\sin\theta, \quad \forall\theta\in[-\pi,\pi]. \end{aligned} \tag{1}$$

Under these boundary conditions, a stress function of Michell's type [8] is proposed for the resin layer ($R_2\leqslant r\leqslant R_3$) as follows:

$$\begin{aligned} \phi=&C_0\theta+C_1r^3\cos\theta+C_2r\theta\sin\theta\\ &+C_3r\ln r\cos\theta+C_4r^{-1}\cos\theta. \end{aligned} \tag{2}$$

From this stress function we derive the stress field

$$\begin{aligned} \sigma_{rr}(r,\theta)&=\frac{1}{r}\frac{\partial\phi}{\partial r}+\frac{1}{r^2}\frac{\partial^2\phi}{\partial\theta^2}\\ &=(2C_1r+2C_2/r+C_3/r-2C_4/r^3)\cos\theta,\\ \sigma_{r\theta}(r,\theta)&=\frac{1}{r^2}\frac{\partial\phi}{\partial\theta}-\frac{1}{r}\frac{\partial^2\phi}{\partial r\,\partial\theta}\\ &=C_0/r^2+(2C_1r+C_3/r-2C_4/r^3)\sin\theta,\\ \sigma_{\theta\theta}(r,\theta)&=\frac{\partial^2\phi}{\partial r^2}=(6C_1r+C_3/r+2C_4/r^3)\cos\theta. \end{aligned} \tag{3}$$

The associated displacement field reads

$$\begin{aligned} u_r(r,\theta)=&\frac{\cos\theta}{2\mu_2}\left[C_1(\kappa_2-2)r^2+\frac{1}{2}((\kappa_2+1)\ln r-1)C_2\right.\\ &\left.+\frac{1}{2}((\kappa_2-1)\ln r-1)C_3+C_4r^{-2}\right]\\ &+\frac{\theta\sin\theta}{2\mu_2}[C_2(\kappa_2-1)+C_3(\kappa_2+1)]+\frac{C_5}{2\mu_2}\cos\theta,\\ u_\theta(r,\theta)=&-\frac{C_0}{2\mu_2}r^{-1}+\frac{\sin\theta}{2\mu_2}\left[C_1(\kappa_2+2)r^2\right.\\ &-\frac{1}{2}((\kappa_2+1)\ln r+1)C_2\\ &\left.-\frac{1}{2}((\kappa_2-1)\ln r+1)C_3+C_4r^{-2}\right]\\ &+\frac{\theta\cos\theta}{2\mu_2}[C_2(\kappa_2-1)+C_3(\kappa_2+1)]\\ &-\frac{C_5}{2\mu_2}\sin\theta+\frac{C_6}{2\mu_2R_3}. \end{aligned} \tag{4}$$

The chapters 8 and 9 in the book of Barber [8] give a detailed presentation of the way in which we have deduced the stress field (3) and displacement field (4) from the stress function (1). For the paper to be self-contained, the Michell stress function method is briefly recalled in Appendix A.

The terms $C_5/(2\mu_2)$ and $C_6/(2\mu_2R_3)$ in (4) represent a horizontal rigid translation and a rigid rotation due to the use of a stress function. The requirement that u_r and u_θ be periodical with respect to θ, i.e.,

$$u_r(r,\theta)=u_r(r,\theta+2\pi), \quad u_\theta(r,\theta)=u_\theta(r,\theta+2\pi),$$

leads to the demand that the terms $\theta\cos\theta$ and $\theta\sin\theta$ in (4) vanish:

$$C_2(\kappa_2-1)+C_3(\kappa_2+1)=0. \tag{5}$$

Using the boundary conditions (1) in (4) while accounting for (5), we obtain a system of linear equations for determining the coefficients C_i ($i=1,2,\ldots,5$):

$$\begin{cases} C_1(\kappa_2-2)R_2^2+\dfrac{C_2}{2}[(\kappa_2+1)\ln R_2-1]\\ \quad+\dfrac{C_3}{2}[(\kappa_2-1)\ln R_2-1]+C_4R_2^{-2}+C_5=2\delta\mu_2,\\ C_1(\kappa_2+2)R_2^2-\dfrac{C_2}{2}[(\kappa_2+1)\ln R_2+1]\\ \quad-\dfrac{C_3}{2}[(\kappa_2-1)\ln R_2+1]+C_4R_2^{-2}-C_5=-2\delta\mu_2,\\ C_1(\kappa_2-2)R_3^2+\dfrac{C_2}{2}[(\kappa_2+1)\ln R_3-1]\\ \quad+\dfrac{C_3}{2}[(\kappa_2-1)\ln R_3-1]+C_4R_3^{-2}+C_5=0,\\ C_1(\kappa_2+2)R_3^2-\dfrac{C_2}{2}[(\kappa_2+1)\ln R_3+1]\\ \quad-\dfrac{C_3}{2}[(\kappa_2-1)\ln R_3+1]+C_4R_3^{-2}-C_5=0,\\ C_2(\kappa_2-1)+C_3(\kappa_2+1)=0,\\ C_0-C_6=0,\\ C_6/R_3-C_0/R_2=2\mu_2\omega R_2. \end{cases} \tag{6}$$

With the notation $\rho = (R_3/R_2)^2$, the solution for the system (6) is given by

$$C_1 = \frac{2\delta\mu_2}{R_2^2(2\rho - \kappa_2^2\rho\ln\rho - 2 - \kappa_2^2\ln\rho)},$$
$$C_2 = \frac{2(\kappa_2+1)(1+\rho)\kappa_2\delta\mu_2}{2\rho - \kappa_2^2\rho\ln\rho - 2 - \kappa_2^2\ln\rho},$$
$$C_3 = -\frac{2(\kappa_2-1)(1+\rho)\kappa_2\delta\mu_2}{2\rho - \kappa_2^2\rho\ln\rho - 2 - \kappa_2^2\ln\rho},$$
$$C_4 = \frac{2R_2^2\rho\kappa_2\delta\mu_2}{2\rho - \kappa_2^2\rho\ln\rho - 2 - \kappa_2^2\ln\rho},$$
$$C_5 = \frac{4\delta\mu_2(\kappa_2(\rho+1)\ln R_3 - \rho)}{2\rho - \kappa_2^2\rho\ln\rho - 2 - \kappa_2^2\ln\rho},$$
$$C_0 = C_6 = -\frac{2\mu_2\omega R_2^2 R_3}{R_3 - R_2}. \tag{7}$$

However the stress field (3) must be in equilibrium with the external forces, i.e the horizontal force P and the moment M with respect to the origin O. Hence, we have

$$\int_{-\pi}^{\pi}(\sigma_{rr}\cos\theta - \sigma_{r\theta}\sin\theta)r\,\mathrm{d}\theta + P = 0,$$
$$\int_{-\pi}^{\pi}\sigma_{r\theta}r^2\,\mathrm{d}\theta + M = 0.$$

These two equations provide

$$C_2 = -\frac{P}{2\pi}, \quad C_0 = -\frac{M}{2\pi}. \tag{8}$$

By combining these two equations with the second and last formulae in (7), we can determine the translation δ and rotation ω in terms of P and M:

$$\delta = \frac{(\kappa_2^2\rho\ln\rho + 2 + \kappa_2^2\ln\rho - 2\rho)}{4\pi(\kappa_2+1)(1+\rho)\kappa_2\mu_2}P, \quad \omega = \frac{(R_3 - R_2)}{4\pi\mu_2 R_2^2 R_3}M, \tag{9}$$

or equivalently,

$$\frac{P}{\delta} = \frac{4\pi(\kappa_2+1)(1+\rho)\kappa_2\mu_2}{\kappa_2^2\rho\ln\rho + 2 + \kappa_2^2\ln\rho - 2\rho}, \quad \frac{M}{\omega R_3^2} = \frac{4\pi\mu_2}{\rho - \sqrt{\rho}}. \tag{10}$$

The terms on the right-hand sides of the foregoing formulae represent the translational stiffness and normalized rotational stiffness, which depend only on the material constants and normalized geometrical parameter ρ.

Then, the other coefficients C_i ($i = 1, 3, 4, 5, 6$) in (3) can be all determined in terms of M and P as follows:

$$C_1 = -\frac{P}{2\pi R_2^2(\kappa_2+1)(1+\rho)\kappa_2},$$
$$C_3 = \frac{(\kappa_2-1)P}{2\pi(\kappa_2+1)}, \quad C_4 = -\frac{\rho P R_2^2}{2\pi(\kappa_2+1)(\rho+1)},$$
$$C_5 = -\frac{P(\kappa_2(\rho+1)\ln R_3 - \rho)}{\pi(\kappa_2+1)(1+\rho)\kappa_2}, \quad C_6 = -\frac{M}{2\pi}. \tag{11}$$

When the contact of the bolt and ring is frictionless, the contact stress vector acting on the contact surface is normal to the latter and passes through the origin, creating a zero moment with respect to it (viz. the moment $M = 0$). Then, the coefficients C_0, C_6 and ω become zero. Generally speaking, the foregoing analytical solution remains valid even for the case where the contact between the bolt and ring is frictional but the bolt does not roll, i.e. the resultant moment of the frictional stresses with respect to the bolt center is null.

3. Numerical simulation and validation

To check the validity of the analytical solution derived above, we apply this solution and use the finite element method (FEM) to make the plane stress analysis of a glass plate of dimension 200 mm × 200 mm × 19 mm with a reinforced pin-loaded joint. The external force is a concentrated force applied at the center of the bolt. The other parameters and conditions used in our analysis are listed below:

- Geometric parameters: $R_0 = 15$ mm, $R_1 = 15$ mm, $R_2 = 30$ mm or 45 mm, $R_3 = 60$ mm, $L = 200$ mm (width and length of the glass plate), $e = 19$ mm (thickness of the glass plate);
- Bolt ($r \leqslant R_0$): $E_0 = 200$ GPa, $\nu_0 = 0.3$;
- Ring ($R_1 \leqslant r \leqslant R_2$): $E_1 = 200$ GPa, $\nu_1 = 0.3$;
- Resin layer ($R_2 \leqslant r \leqslant R_3$): $E_2 = 0.2, 0.5, 1$ or 2 GPa, $\nu_2 = 0.2$;
- Glass plate ($R_3 \leqslant r$ and $|x| \leqslant L/2$ and $|y| \leqslant L/2$): $E_3 = 70$ GPa, $\nu_3 = 0.2$;
- Total force: $F = F_x = 19$ kN applied at the center of the bolt;
- Force per unit thickness: $P = F/e = 1$ kN/mm;
- Boundary conditions: $u_x(x = -L/2, y) = 0$, $u_y(x, y = 0) = 0$;
- Frictionless contact between the bolt and ring: $M = 0$.

Among the above parameters, E_2 varies from 0.2 to 2 GPa and R_2 is equal to 30 or 45 mm.

Table 1
Non-zero coefficients used in the analytical stress solution (Eq. (3)) for the adhesive resin layer

R_2 (mm)	R_3 (mm)	κ_2	P (N/mm)	C_1	C_2	C_3	C_4
45	60	2.333	1000	−3.638E−3	−159.155	63.662	−61879
30	60	2.333	1000	−4.547E−3	−159.155	63.662	−34377

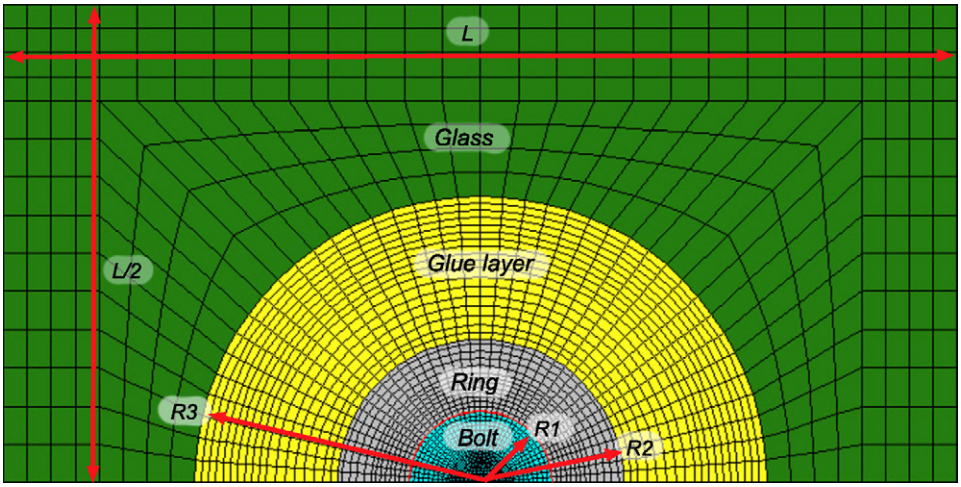

Fig. 4. Mesh of a reinforced pin-loaded joint in a glass structure.

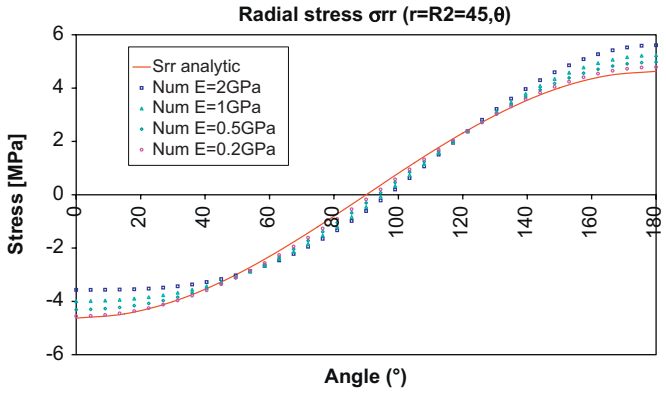

Fig. 5. Normal stress component σ_{rr} at the surface $r = R_2 = 45$ mm.

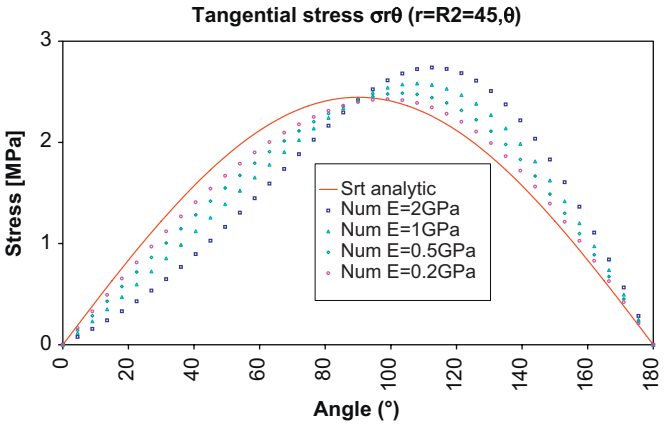

Fig. 6. Tangential stress component $\sigma_{r\theta}$ at the surface $r = R_2 = 45$ mm.

The analytical stress solution for the resin layer of the glass structure under consideration is provided by Eq. (3) in which the expressions of the coefficients C_i are specified by Eq. (10). Since $M = 0$, it is immediate that $C_0 = 0$. The values of the remaining coefficients C_i $(i = 1, 2, 3, 4)$ for the adhesive resin layer are calculated and presented in Table 1. The problem under investigation is linearly elastic, so that, in particular, the coefficients C_i $(i = 1, 2, 3, 4)$ are proportional to the load P with the proportionality constants depending only on the geometrical and material parameters of the resin layer. In addition, according to Eq. (3), for a given radius r, the normal stress components σ_{rr} and $\sigma_{\theta\theta}$ are cosinusoidal functions of θ while the tangent stress component $\sigma_{r\theta}$ is a sinusoidal function of θ. The normal stress σ_{rr} and tangent stress $\sigma_{r\theta}$ acting on the surface between the adhesive resin layer and the steel ring are plotted in Figs. 5, 6, 8 and 9 for $R_2 = 45$ and 30 mm and for the four values of E_2 ranging from 0.2 to 2 GPa. The variation of the corresponding radial stress σ_{rr} along the radial direction is depicted in Figs. 7 and 10.

Next, the glass structure with a pin-loaded joint is analyzed by MSC MARC, a robust Finite Element

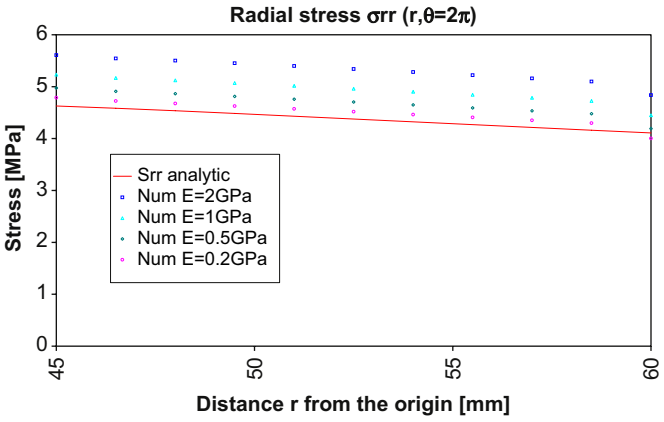

Fig. 7. Radial stress component $\sigma_{rr}(r, \theta = 2\pi)$ with $R_2 < r < R_3$ $(R_2 = 45$ mm).

Program with advanced features for contact problems (see [9]). The mesh of a quarter of the structure, shown in Fig. 4, consists of 2295 in-plane four-node isoparametric elements and comprises 2429 nodes each of which has two degrees of freedom. All the components of the structure are

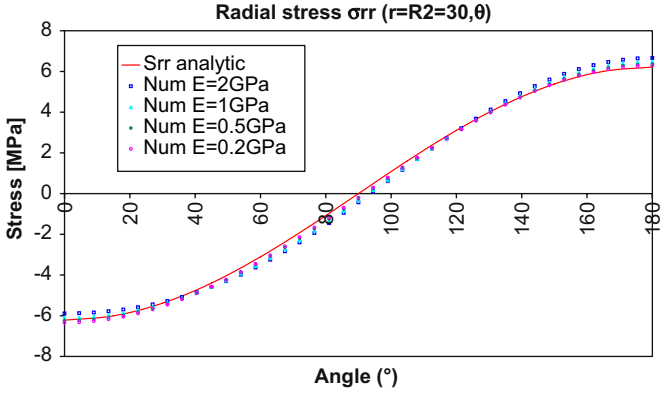

Fig. 8. Normal stress component σ_{rr} at the surface $r = R_2 = 30$ mm.

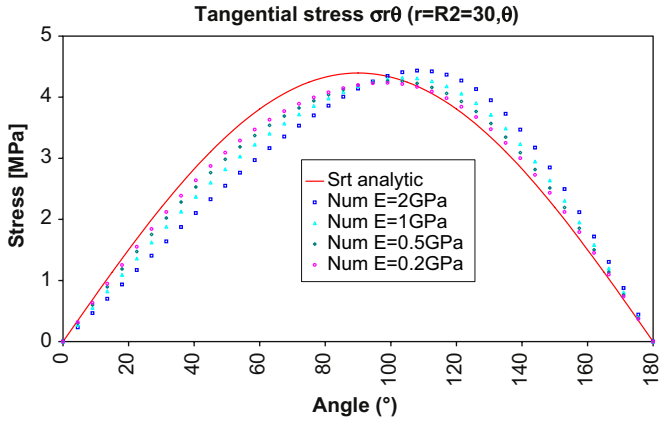

Fig. 9. Tangential stress component $\sigma_{r\theta}$ at the surface $r = R_2 = 30$ mm.

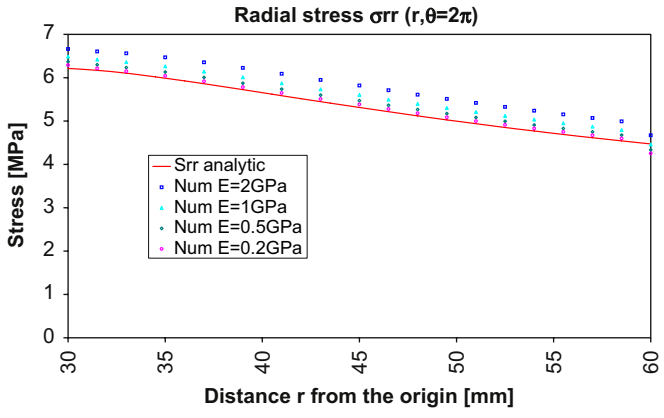

Fig. 10. Radial stress component $\sigma_{rr}(r, \theta = 2\pi)$ with $R_2 < r < R_3$ ($R_2 = 30$ mm).

taken to be deformable. The numerical results for σ_{rr} and $\sigma_{r\theta}$ on the surface between the adhesive resin layer and the steel ring are plotted also in Figs. 5–10 for $R_2 = 45$ and 30 mm. The variation of σ_{rr} along r is shown in Figs. 7 and 10. Furthermore, the distribution of the contact stress on the surface between the steel bolt and ring is illustrated in Figs. 11 and 12 for the aforementioned four values of E_2.

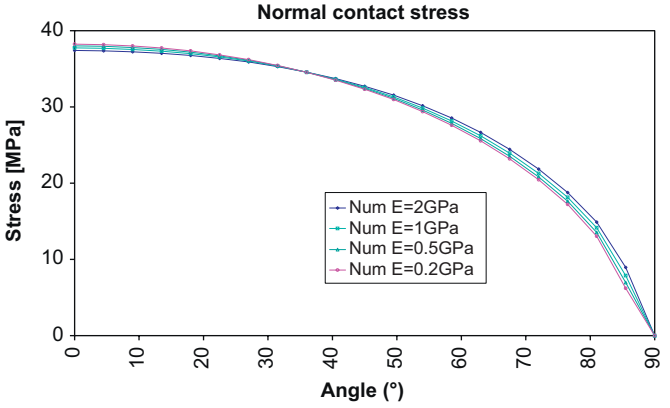

Fig. 11. Normal contact stress on the bolt-ring surface for the case $R_2 = 45$ mm.

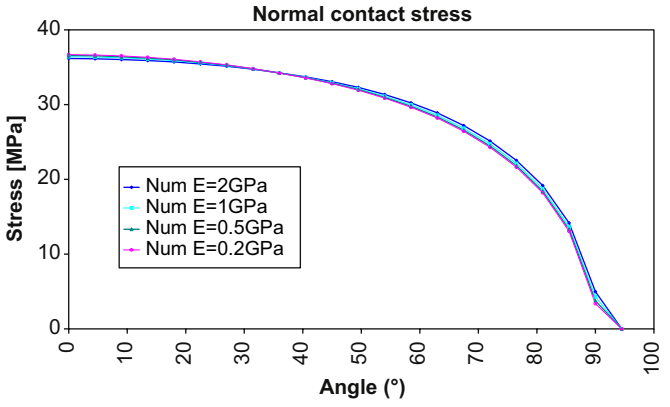

Fig. 12. Normal contact stress on the bolt-ring surface for the case $R_2 = 30$ mm.

Comparing the analytical results and those obtained by FEM, we can draw the following conclusions:

- The analytical solution gives a good approximation for the stress field in the resin. The softer the resin becomes, the analytical solution fits the better the numerical solution (see Figs. 5–10). This conclusion can be extended to the case where the compliance increase has a geometrical origin, for instance, the resin layer becomes thicker.
- The normal contact stress on the surface between the steel bolt and ring is very little sensitive to the change of the resin's stiffness. Consequently, the contact stress determined in the case of a soft adhesive layer can be also be used with a high degree of precision for the case of a stiff adhesive layer.

In this section, we have made the plane stress hypothesis which is appropriate for the real tempered glass structure studied. The conclusions issued from the comparison between the analytical and finite element results hold also for the case of plane strain, since it suffices to replace the

Kolosov constant $\kappa_2 = (3 - \nu_2)/(1 + \nu_2)$ for plane stress by the one $\kappa_2 = 3 - 4\nu_2$ for plane strain.

The analytical solution presented in Section 2 has been compared with the finite element solution by considering a real pin-loaded joint with a non-zero radial force but a zero moment applied at the center of the bolt. If a non-zero moment is involved, the results from the comparison between the analytical solution and the finite element solution are expected to be similar to those presented before.

4. Conclusion

A good knowledge of the stress field inside the thin adhesive resin layer in a pin-loaded joint employed to assemble elements of a tempered glass structure is essential for a safe design of the latter. In this work, an analytical solution has been proposed to determine the stress and displacement fields inside the resin layer on the basis of the fact that the stiffness of a typical resin is much smaller than the one of steel or glass and by using the Michell's stress function method. Our analytical solution has then been compared against and validated by the finite element method for a wide range of resin's rigidity. In particular, it is shown that the difference between the analytical solution and the finite element one is negligible once the resin is sufficiently soft. The analytical results obtained by the present work can be used to predict the first cracking loading of a reinforced pin-loaded joint [10]. They are also useful for obtaining a closed-form solution for the contact stress on the bolt-ring surface (see [10] for details).

Appendix A

In plane (strain or stress) elasticity, the general formula for the stress function in a system of polar coordinates (r, θ) reads

$$\begin{aligned}\phi = {} & A_{01}r^2 + A_{02}r^2\ln(r) + A_{03}\ln(r) + A_{04}\theta \\ & + (A_{11}r^3 + A_{12}r\ln(r) + A_{14}r^{-1})\cos(\theta) + A_{13}r\theta\sin(\theta) \\ & + (B_{11}r^3 + B_{12}r\ln(r) + B_{14}r^{-1})\sin(\theta) + B_{13}r\theta\cos(\theta) \\ & + \sum_{n=2}^{\infty}(A_{n1}r^{n+2} + A_{n2}r^{-n+2} + A_{n3}r^n + A_{n4}r^{-n})\cos(n\theta) \\ & + \sum_{n=2}^{\infty}(B_{n1}r^{n+2} + B_{n2}r^{-n+2} + B_{n3}r^n + B_{n4}r^{-n})\sin(n\theta).\end{aligned} \tag{12}$$

This formula is named after Michell for his first development in 1899. The previous formula of ϕ has the characteristic that each term is a function of separated variables r and θ and satisfies the biharmonic equation in polar coordinate system, i.e

$$\nabla^4\phi = \left(\frac{\partial^2}{\partial r^2} + \frac{1}{r}\frac{\partial}{\partial r} + \frac{1}{r^2}\frac{\partial^2}{\partial\theta^2}\right)\left(\frac{\partial^2\phi}{\partial r^2} + \frac{1}{r}\frac{\partial\phi}{\partial r} + \frac{1}{r^2}\frac{\partial^2\phi}{\partial\theta^2}\right) = 0. \tag{13}$$

Furthermore, the terms corresponding to $\cos n\theta$ or $\sin n\theta$ generate the stress and displacement components also in the form of $\cos n\theta$ or $\sin n\theta$. For example, if $\phi = r^n\cos n\theta$, we shall have the following stress and displacement components

$$\begin{aligned}&\sigma_{rr} = -n(n-1)r^{n-2}\cos n\theta, \\ &\sigma_{r\theta} = n(n-1)r^{n-2}\sin n\theta, \\ &\sigma_{r\theta} = n(n-1)r^{n-2}\cos n\theta, \\ &u_r = -nr^{n-1}\cos n\theta, \quad u_\theta = nr^{n-1}\sin n\theta.\end{aligned} \tag{14}$$

For a detailed presentation, the reader is advised to refer to [8]. In our problem where the displacement boundary conditions are functions of $\cos(0.\theta)$, $\sin(\theta)$ and $\cos(\theta)$ (see Eq. (1)), it is natural to propose the stress function in the simple form

$$\begin{aligned}\phi = {} & C_0\theta + C_1r^3\cos\theta + C_2r\theta\sin\theta \\ & + C_3r\ln r\cos\theta + C_4r^{-1}\cos\theta,\end{aligned} \tag{15}$$

which corresponds to Eq. (2).

References

[1] Rao AK. Elastic analysis of pin joints. Comput Struct 1978;9:125.
[2] Iyer K. Solution for contact in pinned connections. Int J Solid Struct 2001;38:9133.
[3] Mackerle J. Finite element analysis of fastening and joining: a bibliography (1990–2002). Int J Pres Ves Pip 2003;80:253.
[4] Noble B, Hussain MA. Exact solution of certain dual series for indentation and inclusion problems. Int J Eng Sci 1969;7:1149.
[5] Ho KC, Chau KT. An infinite plane loaded by a rivet of a different material. Int J Solid Struct 1997;34:2477.
[6] Chau KT, Wei XX. Stress concentration reduction at a reinforced hole loaded by a bonded circular inclusion. J Appl Mech 2001;68:405.
[7] Ciavarella M, Decuzzi P. The state of stress induced by the plane frictionless cylindrical contact. I. The case of elastic similarity. Int J Solid Struct 2001;38:4507;
Ciavarella M, Decuzzi P. The state of stress induced by the plane frictionless cylindrical contact. II. The general case (elastic dissimilarity). Int J Solid Struct 2001;38:4525.
[8] Barber JR. Elasticity. Kluwer Academic Publisher; 2002.
[9] MSC Software Corporation. MSC MARC Volume A: theory and user information, 2005.
[10] To QD, He Q-C, Cossavella M, Morcant K, Panait A. Closed-form solution for the contact problem of reinforced pin-loaded joints used in glass structures. Int J Solid Struct 2007;44:3887;
To QD, He Q-C, Cossavella M, Morcant K, Panait A, Yvonnet J. Failure analysis of tempered glass structures with pin-loaded joints. Eng Fail Anal 2007;14:841.